



Published in final edited form as:

*J Alzheimers Dis.* 2015 January 1; 44(2): 585–598. doi:10.3233/JAD-141937.

## Atlas-based diffusion tensor imaging correlates of executive function

**Milap A. Nowrangi, M.D., M.Be.<sup>a</sup>, Ozioma Okonkwo, Ph.D.<sup>e</sup>, Constantine Lyketsos, M.D., Kenichi Oishi, M.D., Ph.D.<sup>c</sup>, Susumu Mori, Ph.D.<sup>c</sup>, Marilyn Albert, Ph.D.<sup>b</sup>, and Michelle M. Mielke, Ph.D.<sup>d</sup>**

<sup>a</sup>Department of Psychiatry and Behavioral Sciences, Johns Hopkins University School of Medicine and Johns Hopkins Bayview Medical Center, Baltimore, MD, USA

<sup>b</sup>Department of Neurology, Johns Hopkins University School of Medicine and Johns Hopkins Bayview Medical Center, Baltimore, MD, USA

<sup>c</sup>Department of Radiology, Johns Hopkins University School of Medicine and Johns Hopkins Bayview Medical Center, Baltimore, MD, USA

<sup>d</sup>Department of Health Sciences Research, Division of Epidemiology and Department of Neurology, Mayo Clinic, Rochester, MN, USA

<sup>e</sup>Department of Medicine, University of Wisconsin-Madison, Madison, WI USA

### Abstract

Impairment in executive function (EF) is commonly found in Alzheimer's Dementia (AD) and Mild Cognitive Impairment (MCI). Atlas-based Diffusion Tensor Imaging (DTI) methods may be useful in relating regional integrity to EF measures in MCI and AD.

66 participants (25 NC, 22 MCI, and 19 AD) received DTI scans and clinical evaluation. DTI scans were applied to a pre-segmented atlas and fractional anisotropy (FA) and mean diffusivity (MD) were calculated. ANOVA was used to assess group differences in frontal, parietal, and cerebellar regions. For regions differing between groups ( $p < 0.01$ ), linear regression examined the relationship between EF scores and regional FA and MD.

Anisotropy and diffusivity in frontal and parietal lobe white matter (WM) structures were associated with EF scores in MCI and only frontal lobe structures in AD. EF was more strongly associated with FA than MD. The relationship between EF and anisotropy and diffusivity was strongest in MCI. These results suggest that regional WM integrity is compromised in MCI and AD and that FA may be a better correlate of EF than MD.

### Keywords

Executive Function; DTI; Alzheimer's disease; MCI

---

Corresponding Author for Proofs and Reprints: <sup>a</sup>Milap A. Nowrangi, M.D., M.Be., Department of Psychiatry, Johns Hopkins Bayview Medical Center, 5300 Alpha Commons Drive, 4<sup>th</sup> Floor, Baltimore, MD 21224, Office: 410-550-2294, FAX: 410-550-1407, mnowran1@jhmi.edu.

Its contents are solely the responsibility of the authors and do not necessarily represent the official view of NIH.

## 1.1 Introduction

Alzheimer's Dementia (AD) is the result of a neurodegenerative disease clinically characterized primarily by progressive cognitive decline. While memory impairment has received the most focus, executive function (EF) deficits are frequently present in persons with mild cognitive impairment (MCI) and AD [1–7]. Impairment in EF is a key component of functional decline and disability in both MCI and AD [8–16] and, as such, has recently become the focus of more intense neurobiological research. EF refers to a broad category of cognitive skills commonly thought of as “higher order” or “supervisory,” whose role is to control and coordinate other cognitive faculties like language, memory, visuospatial ability, and praxis [17]. EF is thought to be associated with frontal and posterior brain regions, including the parietal lobes, and the cingulate cortex. [1, 2, 6, 18] Also of note, the cerebellar lobes are well-known to be associated with cognitive function, particularly executive functions including working memory, multi-tasking, and inhibition. [19] Few studies have examined the relationship between these brain regions and progressive EF deficits over the clinical course of AD.

Diffusion Tensor Imaging (DTI) is an imaging technique for the *in vivo* measurement of the white matter (WM) microstructural organization [20–22]. Fractional anisotropy (FA) and mean diffusivity (MD) are two measures used to quantify the integrity of WM microstructure by measuring the degree of anisotropy or magnitude of water diffusion in cerebral tissue, respectively [23–26]. Pre-segmented, atlas-based methods are promising approaches of examining a larger number of 3D-ROIs with high resolution [27–30].

While DTI is a potential tool for the early detection of AD, more research is needed to understand the utility of measuring white matter to elucidate the neural underpinnings of cognitive abilities. In the present study we used an atlas-based DTI method to investigate cross-sectional relationships between common tests of EF and multiple brain regions in cognitively normal controls (NC), and in MCI and AD participants. We hypothesized that the EF measures would associate with FA and MD in both frontal and posterior (parietal and cerebellar) regions. We also hypothesized that relationships between EF and FA and MD would be most evident in MCI patients, compared to AD or NC, because they represent a more heterogeneous and cognitively dynamic cohort with increased variability in cognitive and biological measurement.

## 1.2 Methods

### 1.2.1 Participants and study design

Participants included well-characterized community-dwelling volunteers enrolled in a study examining the utility of anisotropy and diffusivity measurements as biomarkers of AD progression. Study methods have previously been described in detail [31]. Briefly, participants were recruited through the Clinical Core of the Johns Hopkins Alzheimer's Disease Research Center and associated Johns Hopkins clinics. Evaluations included medical, neurological, and psychiatric examinations. All participants received an extensive neuropsychological battery. Additionally, each participant received a MRI scan (detailed

below) and provided a blood sample. Based on this clinical information (excluding imaging), diagnoses of NC, MCI, or AD were made as follows. NC participants had a Clinical Dementia Rating (CDR) [32, 33] of 0. Participants with *amnestic* Mild Cognitive Impairment (MCI) were non-demented, had mild memory problems, a CDR = 0.5, and met Mayo criteria for amnestic MCI, single or multiple domains [34]. Mild AD participants had a CDR = 1 and met NINCDS-ADRDA criteria for probable AD [35]. All participants were >55 years of age, had no history of a neuropsychiatric disease other than AD, and had an informant who could provide information about their daily function. Informed consent was obtained prior to the initiation of the study in accordance with the requirements of the Johns Hopkins Institutional Review Board. Consent followed guidelines endorsed by the Alzheimer's Association for participation of cognitively impaired individuals.

### 1.2.2 DTI scan acquisition and image processing

For each participant, a DTI, co-registered, double-echo fast spin echo (DE-FSE) was acquired using a 3T scanner (Gyrosan NT, Philips Medical Systems). The scanning parameters were as follows. DTI: single-shot echo-planar imaging; 30 diffusion weighting orientations; b-value 700 s/mm<sup>2</sup>; 50–60 gapless whole-brain axial sections of 2.2 mm thickness; matrix 96 × 96; field of view (FOV) 212 mm × 212 mm; zero-filled to 256 mm × 256 mm. DE-FSE: first echo time (TE) 10.1 ms; second TE 96.0 ms; repetition time (TR) 3,000 ms; 48 gapless whole-brain axial slices of 3 mm thickness; matrix 256 × 247; FOV 240 mm × 210 mm; zero-filled to 256 mm × 256 mm. After the raw diffusion-weighted images were corrected for motion, eddy current, and B0-susceptibility distortion [36], a tensor field was calculated. All images were co-registered and re-sliced to 1 mm isotropic resolution (181 × 217 × 181 matrix). The software used for DTI image processing was DtiStudio (lbam.med.jhmi.edu or [www.MriStudio.org](http://www.MriStudio.org)). [37]

### 1.2.3 Normalization of the images to the JHU-MNI atlas, tissue segmentation, and parcellation of gray and white matter

The DTI was normalized to a JHU-MNI “eve” atlas, as previously described [38]. Briefly, DTI was first transformed using a 12-parameter affine transformation and then large deformation diffeomorphic metric mapping (LDDMM). From the normalized tensor field, FA and MD were calculated. The boundary of the cortex and WM was defined by an FA threshold of 0.25 after normalization. While this approach allows imaging of the detailed white matter anatomy of the participant, it also contains participant-specific anatomical features in the superficially located white matter. The methodological detail of the image transformation using LDDMM and the application to Alzheimer's disease with substantial brain atrophy has been previously reported in which we demonstrated high registration accuracy for both normal elderly and Alzheimer's disease individuals. Fig. 1 illustrates the normalization procedure. [29]

After image normalization and parcellation of gray and white matter, the JHU-MNI “eve” atlas (<http://cmrm.med.jhmi.edu/> or <http://www.slicer.org/publications/item/view/1883>) was overlaid on each normalized image. The atlas contains 24 cortical areas and 50 subcortical areas in each hemisphere. In the FA analysis, 24 cortical areas were further subdivided into

gray and white matter regions, resulting in a total of 196 cortical and subcortical regions over both hemispheres.

#### 1.2.4 Selection of neuropsychological measures of executive functioning (EF)

Participants received extensive neuropsychological testing at baseline including tests of episodic memory, language, and EF. Tests of EF included Trails Making Test (TMT) Parts A and B, and category (animals and vegetables) and letter (“F”, “A”, and “S”) verbal fluency. TMT A and B jointly assess attention, visual scanning and search skills, and psychomotor speed and coordination. [39]. Independently, TMT A assesses processing speed whereas TMT B assesses set switching therefore, both were included in the analysis. The category and letter fluency tasks evaluated semantic and phonemic verbal fluency, respectively [40]. Scores on each test were converted to Z scores using means and standard deviations from the NC group, and then averaged to create an EF composite. Subsequent statistical analyses were performed using this composite measure.

#### 1.2.5 Statistical analysis

Differences in baseline characteristics between NC, MCI, and AD groups were examined using Fisher’s Exact Tests for categorical variables and ANOVAs for continuous variables, with t-tests for pairwise comparisons when a significant difference ( $p < 0.05$ ) was noted.

In order to test our hypothesis, and to limit the number of candidate regions examined, we first identified the frontal, parietal, and cerebellar lobes as broad lobar regions of interest. We chose these regions because current literature has supported their role in EF [1, 2, 6, 18]. We selected the pons as a control region because it is not known to subserve EF and is typically not affected in AD. We identified the 26 FA and 46 MD substructures that are localizable using our atlas-based method. We next used ANOVA to examine whether FA and MD in these ROIs differed between NC, MCI, and AD. Given the multiple areas, we used  $p < 0.01$  as our significance level for the three-group comparison via ANOVA. For all areas meeting this level, we then conducted all two-way group comparisons using a Bonferroni correction within each area with significant group differences. In further analyses, we conducted multivariate linear regression models, adjusting for age and education (based on the literature) in-group to examine the association between EF and FA and MD of each ROI.

All computations were done using STATA version 11.0 (StataCorp, College Station, TX).

### 1.3 Results

#### 1.3.1 Participant characteristics

A total of 75 participants were originally recruited (25 NC, 25 MCI, and 25 AD). Images that did not satisfy the quality required for whole brain LDDMM, however, were omitted resulting in 25 NC, 22 MCI, and 19 AD for the present analyses. There were no differences between groups with regards to age, sex, or education [31]. As expected, AD participants were more cognitively impaired than those with MCI or NC on the MMSE, CDR-Global

and CDR sum of boxes, and other neuropsychological tests, including those measuring EF (Table 1).

### 1.3.2 Group differences on FA and MD

In the FA analyses, 8 structures significantly differed between diagnostic groups (Table 2). Four localized to the frontal lobes and the remaining 4 localized to the parietal lobes. The frontal structures included: bilateral middle frontal gyri white matter, left superior frontal gyrus white matter, and right inferior frontal gyrus white matter, and left lateral fronto-orbital gyrus white matter. The parietal structures that differed between groups included: bilateral superior parietal gyrus white matter and bilateral angular gyrus white matter. There were no group differences found within the cerebellar lobes.

In the MD analyses, 12 structures significantly differed between groups: 7 structures within the frontal lobes, one within the parietal lobe, and three in the cingulate gyrus, which spans the frontal and parietal lobes (Table 3). For the frontal lobe, the following structures differed significantly: bilateral middle frontal gyri white matter, bilateral gyrus rectus, left superior and inferior frontal gyri white matter, and the left lateral fronto-orbital gyrus. The only parietal lobe structure found to differ between groups was the right angular gyrus. Lastly, the bilateral cingulate gyrus white matter and left cingulate gyrus were also found to differ between groups. The cerebellum was not found to differ significantly between groups for either FA or MD.

### 1.3.3 Associations between FA, MD, and EF

We next examined the association between FA or MD in each of the ROIs found to differ between diagnostic group and EF Z-scores using multivariate linear regression, and controlling for age and education. For the FA analyses, there was no association between FA in any ROI and EF Z-scores among the NC. However, within the MCI group, higher FA values in the left superior and middle frontal gyrus white matter, right inferior frontal and parietal lobe angular gyrus white matter were significantly associated with higher EF Z-scores. Among AD subjects, higher FA values in the left superior frontal white matter, right middle and inferior frontal gyri white matter were also associated with higher EF Z-scores. These findings are shown in Table 4.

There were no associations between MD in any ROI and EF Z-scores among NC or AD patients. Among MCI patients, there was only one statistically significant association such that higher MD in the right cingulate gyrus white matter was associated with lower EF z-scores.

## 1.4 Discussion

In this DTI study of NC, MCI, and AD participants, we examined the relationship between regional WM integrity (FA and MD) and measures of EF. We tested the hypothesis that loss of integrity in specific areas of the frontal and posterior (parietal and cerebellum) brain WM was associated with worse performance on tests of EF. We also hypothesized that this regional distribution would be most evident in the MCI group compared to AD or NC. We found 8 structures in the FA analyses and 12 in the MD analyses that differed between

diagnostic groups. When examining FA, significant relationships with EF performance were only found within frontal white matter among AD patients, and with both frontal and parietal white matter within the MCI group – a finding that supported our initial hypothesis that the association between EF and brain region would be strongest in the MCI group. For the MD analysis, the only significant EF correlation was with the right cingulate gyrus white matter within the AD group. Though the cerebellar lobes were included because of their importance in executive cognition, there was no significant group discriminability so they were not carried forward in the regression analysis.

The results of this study add to findings from other studies that examined relationships between non-atlas-based (ROI) DTI measurements and cognitive test performance. For example, though they only compared AD to NC, Sjöbeck, et al. [41] found that reduced performance on executive functioning measures correlated with frontal FA WM changes (MD was not assessed). Another study [42] examined the relationship between FA and two measures of diffusivity in normal appearing white matter and cognitive ability. They found that frontal FA and radial diffusivity (DR) associated best with EF while parietal DR was associated with visuospatial ability. However, the analysis was not stratified by group. Chen, et al. [43] examined the associations between FA and MD in the periventricular white matter (PVWM) and EF performance. They found that frontal PVWM was associated with performance on a verbal fluency test, the Wisconsin Card Sorting Test (WCST), and TMT B, while parietal PVWM was associated with perseverative errors on the WCST and TMT A. However, in this study, patients with MCI and AD were combined to increase statistical power.

Recent research has suggested that networks of brain regions connected by white matter tracts in a cortico-cortical fashion underpin EF specifically. In AD, impaired executive function is an early and important feature of the disease [44, 45]. Through the effects of the neurodegenerative process on several regions over time, it is hypothesized that the EF network is disrupted resulting in the cognitive deficits of AD. In as much as MCI reflects a lesser amount of pathological burden compared to AD, one might expect there to be less integrity loss and accordingly a more preserved network where both anterior and posterior regions are more preserved. Recent research using fMRI has elaborated the structure and function of this purported network where several regions of activity have been related to impaired tests of EF in different clinical populations [46–49]. Similarly, structural MRI has revealed both anterior and posterior (parietal) areas of cortical volume change consistent with performance on measures of EF in subjects with MCI and AD [1, 2]. Therefore, MCI can be thought of as a stage with less impairment cognitively and pathologically compared to AD and the results of this study add that microstructural integrity of the regions belonging to this network may also be an indicator of disease evolution. The results of this study, though not derived from an analysis of the integrity of the EF “network” as a whole suggests that specific anterior and posterior brain regions follow previously identified regional and network-related differences between diagnostic groups. Further research is needed to tie together these regions with such techniques as functioning imaging and structural tractography.



In the present study, we found that FA was more strongly associated with EF performance than MD. The difference between anisotropy and diffusivity and, specifically, what each represents is becoming an important topic as DTI technology continues to mature and is applied to clinical populations. The results from our previous published work [31, 50], have found that MD measurements are a better indicator of cross-sectional and longitudinal anatomic white-matter change while FA is more strongly associated with cognitive change. Interpretation of this is cautioned largely because evaluation of the diffusion tensor and FA, in particular, is complex. Image noise, artifacts (e.g. head motion), partial volume averaging effects, and regions of crossing white matter fibers all potentially serve to confound simple interpretation of FA values. In the absence of these challenges, however, FA is a highly sensitive but nonspecific biomarker of microstructural architecture [51]. As a result, recent DTI research has also calculated mean, axial (parallel), and radial (perpendicular) diffusivities to provide more specific information about the diffusion tensor to be used in conjunction with FA measures.

Most studies employ either voxel-based or region of interest (ROI)-based approaches to quantify the DTI-derived measures for further statistical analyses. While these methods have been useful for revealing abnormalities of specific WM tracts related to diseases, their application to studies correlating structure and function are not straightforward. A limitation of voxel-based methods is the low signal-to-noise ratio that results in lower sensitivity to detect mild, but widespread, anatomical alterations related to neurocognitive functions [52]. The ROI-based approach can reasonably group voxels following anatomical structures with specific functions, although multiple 3D-ROIs are required to extract maximum information from multiple brain structures related to EF [53]. To perform whole brain analysis with no *a priori* hypothesis, voxel-based analysis is one of the most widely used approaches. However, this approach tends to miss the widely distributed regions that show only small changes in the parameters [52]. Structure-based voxel grouping, such as atlas-based analysis (ABA) [54] that was used in our study, is one of the attempts to overcome such limitation, based on the hypothesis that the white matter pathology of AD is structure-specific. The unique aspect of our approach is an implementation of the JHU-brain parcellation map, which is an only DTI atlas with fine delineation of DTI-visible white matter structures. If we hypothesize that the white matter pathology of AD is tract-specific, we may apply tract-based voxel grouping, such as Tract-Based Spatial Statistics (TBSS) [55].

This study has several limitations. First, we acknowledge that we did not complete a full executive functioning battery. Instead, we included tests from the neuropsychological battery given in this study that are thought to represent elements of EF (TMT A and B, and verbal fluency). Future work from our group will employ a wider range of executive measures for analysis. Second, the atlas used in this study was not able to fully characterize medial frontal lobe structures. Specifically, regions of the prefrontal cortex (specifically orbito-frontal, dorso-lateral, and ventrolateral) have been highly regarded as active during executive processes, a finding that has been substantiated in other neuroimaging, particularly fMRI, literature [56, 57]. As atlas methods continue to develop, we hope that medial frontal structures, given their high level of interconnectivity, will become more analyzable with this method. Moreover, the lack of group discrimination within the cerebellar lobes that

prevented further statistical analysis can be thought of as a consequence of the previously discussed imaging limitations. Moreover, the smaller size of the cerebellum relative to the frontal and parietal lobes may have limited the detection of white matter changes. This may also indicate that the cerebellum is not preferentially affected with respect to white matter changes in MCI and AD. Further research into cerebellar white matter in aging and dementia will be important moving forward. Next, while our approach utilized a method (atlas-based) to afford a larger number of analyzable regions, we still in effect, utilized an ROI approach based on an *a priori* hypothesis that EF was related to frontal, parietal, and cerebellar regions. While this may be construed as a weakness, it could also be seen as a strength where this research is less exploratory and more hypothesis driven. Ultimately, we suggest that the most effective methods for this type of work will be multi-method. Finally, the use of the same contrasts for registration and subsequent analysis might raise a fundamental issue for all registration-based image analysis. In our analysis, if a patient has lowered FA in a specific white matter area, the segmentation results may lead to smaller volume of the area due to the FA decrease. This type of anatomy-intensity coupling is an important limitation and we need to be careful when we interpret the data. [58]

In summary, this is the first known study utilizing an atlas-based DTI method to associate executive function with brain WM integrity in NC, MCI, and AD participants. We provide evidence that the MCI group exhibited the strongest relationships in frontal and parietal brain regions. This finding is in line with current literature, though using other methods, that also suggest that frontal as well as posterior brain regions are involved in EF processes. Moreover, our findings indicate that FA may be a better marker of functional (cognitive) change than MD, but continued research in this area is necessary.

## Acknowledgments

This publication was made possible by grants from the National Institutes of Health (NIH): RO1AG020012, R21AG033774, P41EB015909, and P50AG005146.

## References

1. Chang YL, Jacobson MW, Fennema-Notestine C, Hagler DJ, Jennings RG, Dale AM, McEvoy LK. Level of Executive Function Influences Verbal Memory in Amnesic Mild Cognitive Impairment and Predicts Prefrontal and Posterior Cingulate Thickness. *Cerebral Cortex*. 2010; 20:1305–1313. [PubMed: 19776343]
2. Dickerson BC, Wolk DA. Dysexecutive versus amnesic phenotypes of very mild Alzheimer's disease are associated with distinct clinical, genetic and cortical thinning characteristics. *Journal of Neurology, Neurosurgery & Psychiatry*. 2010; 82:45–51.
3. McDonald CR, Gharapetian L, McEvoy LK, Fennema-Notestine C, Hagler DJ, Holland D, Dale AM. Relationship between regional atrophy rates and cognitive decline in mild cognitive impairment. *NBA*. 2011:1–12.
4. Pa J, Boxer A, Chao LL, Gazzaley A, Freeman K, Kramer J, Miller BL, Weiner MW, Neuhaus J, Johnson JK. Clinical-neuroimaging characteristics of dysexecutive mild cognitive impairment. *Annals of Neurology*. 2009; 65:414–423. [PubMed: 19399879]
5. Royall DR, Lauterbach EC, Cummings JL, Reeve A, Rummans TA, Kaufer DI, LaFrance WC Jr, Coffey CE. Executive control function: a review of its promise and challenges for clinical research. A report from the Committee on Research of the American Neuropsychiatric Association. *J Neuropsychiatry Clin Neurosci*. 2002; 14:377–405. [PubMed: 12426407]



6. Stricker NH, Chang YL, Fennema-Notestine C, Delano-Wood L, Salmon DP, Bondi MW, Dale AM. Distinct profiles of brain and cognitive changes in the very old with Alzheimer disease. *Neurology*. 2011; 77:713–721. [PubMed: 21832223]
7. Stopford CL, Thompson JC, Neary D, Richardson AMT, Snowden JS. Working memory, attention, and executive function in Alzheimer's disease and frontotemporal dementia. *Cortex*. 2011:1–18.
8. Kavcic V, Ni H, Zhu T, Zhong J, Duffy CJ. White matter integrity linked to functional impairments in aging and early Alzheimer's disease. *Alzheimers Dement*. 2008; 4:381–389. [PubMed: 19012862]
9. Marshall GA, Rentz DM, Frey MT, Locascio JJ, Johnson KA, Sperling RA. Executive function and instrumental activities of daily living in mild cognitive impairment and Alzheimer's disease. *Alzheimers Dement*. 2011; 7:300–308. [PubMed: 21575871]
10. Aretouli E, Brandt J. Everyday functioning in mild cognitive impairment and its relationship with executive cognition. *Int J Geriatr Psychiatry*. 2010; 25:224–233.
11. Baddeley AD, Bressi S, Della Sala S, Logie R, Spinnler H. The decline of working memory in Alzheimer's disease. A longitudinal study. *Brain*. 1991; 114 (Pt 6):2521–2542. [PubMed: 1782529]
12. Barberger-Gateau P, Fabrigoule C. Re: Bell-McGinty et al standard measures of executive function in predicting instrumental activities of daily living in older adults. *Int J Geriatr Psychiatry*. 2003; 18:459–460. [PubMed: 12766926]
13. Bell-McGinty S, Podell K, Franzen M, Baird AD, Williams MJ. Standard measures of executive function in predicting instrumental activities of daily living in older adults. *Int J Geriatr Psychiatry*. 2002; 17:828–834. [PubMed: 12221656]
14. Boyle PA, Malloy PF, Salloway S, Cahn-Weiner DA, Cohen R, Cummings JL. Executive dysfunction and apathy predict functional impairment in Alzheimer disease. *Am J Geriatr Psychiatry*. 2003; 11:214–221. [PubMed: 12611751]
15. Cahn-Weiner DA, Boyle PA, Malloy PF. Tests of executive function predict instrumental activities of daily living in community-dwelling older individuals. *Appl Neuropsychol*. 2002; 9:187–191. [PubMed: 12584085]
16. Fischer P, Jungwirth S, Zehetmayer S, Weissgram S, Hoenigschnabl S, Gelpi E, Krampla W, Tragl KH. Conversion from subtypes of mild cognitive impairment to Alzheimer dementia. *Neurology*. 2007; 68:288–291. [PubMed: 17242334]
17. Miyake A, Friedman NP, Emerson MJ, Witzki AH, Howerter A, Wager TD. The unity and diversity of executive functions and their contributions to complex “Frontal Lobe” tasks: a latent variable analysis. *Cogn Psychol*. 2000; 41:49–100. [PubMed: 10945922]
18. Eslinger PJ, Moore P, Anderson C, Grossman M. Social cognition, executive functioning, and neuroimaging correlates of empathic deficits in frontotemporal dementia. *The Journal of neuropsychiatry and clinical neurosciences*. 2011; 23:74–82. [PubMed: 21304142]
19. Buckner RL. The cerebellum and cognitive function: 25 years of insight from anatomy and neuroimaging. *Neuron*. 2013; 80:807–815. [PubMed: 24183029]
20. Basser PJ, Jones DK. Diffusion-tensor MRI: theory, experimental design and data analysis - a technical review. *NMR Biomed*. 2002; 15:456–467. [PubMed: 12489095]
21. Beaulieu C, Does MD, Snyder RE, Allen PS. Changes in water diffusion due to Wallerian degeneration in peripheral nerve. *Magn Reson Med*. 1996; 36:627–631. [PubMed: 8892217]
22. Mori S, Crain BJ, Chacko VP, van Zijl PC. Three-dimensional tracking of axonal projections in the brain by magnetic resonance imaging. *Ann Neurol*. 1999; 45:265–269. [PubMed: 9989633]
23. Arfanakis K, Houghton VM, Carew JD, Rogers BP, Dempsey RJ, Meyerand ME. Diffusion tensor MR imaging in diffuse axonal injury. *AJNR Am J Neuroradiol*. 2002; 23:794–802. [PubMed: 12006280]
24. Pierpaoli C, Jezzard P, Basser PJ, Barnett A, Di Chiro G. Diffusion tensor MR imaging of the human brain. *Radiology*. 1996; 201:637–648. [PubMed: 8939209]
25. Song SK, Kim JH, Lin SJ, Brendza RP, Holtzman DM. Diffusion tensor imaging detects age-dependent white matter changes in a transgenic mouse model with amyloid deposition. *Neurobiol Dis*. 2004; 15:640–647. [PubMed: 15056472]

26. Harsan LA, Poulet P, Guignard B, Steibel J, Parizel N, de Sousa PL, Boehm N, Grucker D, Ghandour MS. Brain dysmyelination and recovery assessment by noninvasive in vivo diffusion tensor magnetic resonance imaging. *J Neurosci Res.* 2006; 83:392–402. [PubMed: 16397901]
27. Oishi, K. Multi-modal MRI analysis with disease-specific spatial filtering: initial testing to predict mild cognitive impairment patients who convert to Alzheimer's disease. 2011. p. 1-8.
28. Mori S, Oishi K, Jiang H, Jiang L, Li X, Akhter K, Hua K, Faria AV, Mahmood A, Woods R, Toga AW, Pike GB, Neto PR, Evans A, Zhang J, Huang H, Miller MI, van Zijl P, Mazziotta J. Stereotaxic white matter atlas based on diffusion tensor imaging in an ICBM template. *Neuroimage.* 2008; 40:570–582. [PubMed: 18255316]
29. Oishi K, Faria A, Jiang H, Li X, Akhter K, Zhang J, Hsu JT, Miller MI, van Zijl PC, Albert M, Lyketos CG, Woods R, Toga AW, Pike GB, Rosa-Neto P, Evans A, Mazziotta J, Mori S. Atlas-based whole brain white matter analysis using large deformation diffeomorphic metric mapping: application to normal elderly and Alzheimer's disease participants. *Neuroimage.* 2009; 46:486–499. [PubMed: 19385016]
30. Sullivan EV, Pfefferbaum A. Diffusion tensor imaging in normal aging and neuropsychiatric disorders. *Eur J Radiol.* 2003; 45:244–255. [PubMed: 12595109]
31. Mielke MM, Kozauer NA, Chan KCG, George M, Toroney J, Zerrate M, Bandeen-Roche K, Wang M-C, Vanzijl P, Pekar JJ, Mori S, Lyketos CG, Albert M. Regionally-specific diffusion tensor imaging in mild cognitive impairment and Alzheimer's disease. *NeuroImage.* 2009; 46:47–55. [PubMed: 19457371]
32. Hughes CP, Berg L, Danziger WL, Coben LA, Martin RL. A new clinical scale for the staging of dementia. *Br J Psychiatry.* 1982; 140:566–572. [PubMed: 7104545]
33. Morris JC. The Clinical Dementia Rating (CDR): current version and scoring rules. *Neurology.* 1993; 43:2412–2414. [PubMed: 8232972]
34. Petersen RC. Mild cognitive impairment as a diagnostic entity. *J Intern Med.* 2004; 256:183–194. [PubMed: 15324362]
35. McKhann G, Drachman D, Folstein M, Katzman R, Price D, Stadlan EM. Clinical diagnosis of Alzheimer's disease: report of the NINCDS-ADRDA Work Group under the auspices of Department of Health and Human Services Task Force on Alzheimer's Disease. *Neurology.* 1984; 34:939–944. [PubMed: 6610841]
36. Huang H, Ceritoglu C, Li X, Qiu A, Miller MI, van Zijl PC, Mori S. Correction of B0 susceptibility induced distortion in diffusion-weighted images using large-deformation diffeomorphic metric mapping. *Magn Reson Imaging.* 2008; 26:1294–1302. [PubMed: 18499384]
37. Jiang H, van Zijl PC, Kim J, Pearlson GD, Mori S. DtiStudio: resource program for diffusion tensor computation and fiber bundle tracking. *Comput Methods Programs Biomed.* 2006; 81:106–116. [PubMed: 16413083]
38. Oishi K, Faria A, Jiang H, Li X, Akhter K, Zhang J, Hsu JT, Miller MI, van Zijl PCM, Albert M, Lyketos CG, Woods R, Toga AW, Pike GB, Rosa-Neto P, Evans A, Mazziotta J, Mori S. Atlas-based whole brain white matter analysis using large deformation diffeomorphic metric mapping: application to normal elderly and Alzheimer's disease participants. *NeuroImage.* 2009; 46:486–499. [PubMed: 19385016]
39. Reitan RM. The relation of the trail making test to organic brain damage. *J Consult Psychol.* 1955; 19:393–394. [PubMed: 13263471]
40. Lezak, MD. Verbal functions and language skills. In: Lezak, MD., editor. *Neuropsychological Assessment.* Oxford University Press: Oxford: 2004c.
41. Sjöbeck M, Elfgrén C, Larsson E-M, Brockstedt S, Lätt J, Englund E, Passant U. Alzheimer's disease (AD) and executive dysfunction. A case-control study on the significance of frontal white matter changes detected by diffusion tensor imaging (DTI). *Archives of Gerontology and Geriatrics.* 2010; 50:260–266. [PubMed: 19419776]
42. Huang J, Friedland RP, Auchus AP. Diffusion tensor imaging of normal-appearing white matter in mild cognitive impairment and early Alzheimer disease: preliminary evidence of axonal degeneration in the temporal lobe. *AJNR Am J Neuroradiol.* 2007; 28:1943–1948. [PubMed: 17905894]

43. Chen T-F, Chen Y-F, Cheng T-W, Hua M-S, Liu H-M, Chiu M-J. Executive dysfunction and periventricular diffusion tensor changes in amnesic mild cognitive impairment and early Alzheimer's disease. *Human Brain Mapping*. 2009; 30:3826–3836. [PubMed: 19441023]
44. Carlson MC, Xue QL, Zhou J, Fried LP. Executive decline and dysfunction precedes declines in memory: the Women's Health and Aging Study II. *J Gerontol A Biol Sci Med Sci*. 2009; 64:110–117. [PubMed: 19182230]
45. Kavcic V, Ni H, Zhu T, Zhong J, Duffy C. White matter integrity linked to functional impairments in aging and early Alzheimer's disease. *Alzheimer's and Dementia*. 2008; 4:381–389.
46. Connolly CG, Foxe JJ, Nierenberg J, Shpaner M, Garavan H. The neurobiology of cognitive control in successful cocaine abstinence. *Drug and alcohol dependence*. 2012; 121:45–53. [PubMed: 21885214]
47. Schmitz N, Arkink EB, Mulder M, Rubia K, Admiraal-Behloul F, Schoonmann GG, Kruit MC, Ferrari MD, van Buchem MA. Frontal lobe structure and executive function in migraine patients. *Neuroscience Letters*. 2008; 440:92–96. [PubMed: 18556120]
48. Schmitz N, Rubia K, Daly E, Smith A, Williams S, Murphy DGM. Neural correlates of executive function in autistic spectrum disorders. *BPS*. 2006; 59:7–16.
49. Wilsmeier A, Ohrmann P, Suslow T, Siegmund A, Koelkebeck K, Rothermundt M, Kugel H, Arolt V, Bauer J, Pedersen A. Neural correlates of set-shifting: decomposing executive functions in schizophrenia. *Journal of psychiatry & neuroscience: JPN*. 2010; 35:321–329. [PubMed: 20731964]
50. Nowrangi MA, Lyketsos CG, Leoutsakos JM, Oishi K, Albert M, Mori S, Mielke MM. Longitudinal, region-specific course of diffusion tensor imaging measures in mild cognitive impairment and Alzheimer's disease. *Alzheimers Dement*. 2012
51. Alexander AL, Lee JE, Lazar M, Field AS. Diffusion tensor imaging of the brain. *Neurotherapeutics*. 2007; 4:316–329. [PubMed: 17599699]
52. Davatzikos C. Why voxel-based morphometric analysis should be used with great caution when characterizing group differences. *NeuroImage*. 2004; 23:17–20. [PubMed: 15325347]
53. Oishi K, Mielke MM, Albert M, Lyketsos CG, Mori S. DTI analyses and clinical applications in Alzheimer's disease. *J Alzheimers Dis*. 2011; 26(Suppl 3):287–296. [PubMed: 21971468]
54. Oishi K, Faria A, Jiang H, Li X, Akhter K, Zhang J, Hsu JT, Miller MI, van Zijl PC, Albert M, Lyketsos CG, Woods R, Toga AW, Pike GB, Rosa-Neto P, Evans A, Mazziotta J, Mori S. Atlas-based whole brain white matter analysis using large deformation diffeomorphic metric mapping: application to normal elderly and Alzheimer's disease participantstlas. *Neuroimage*. 2009; 46:486–499. [PubMed: 19385016]
55. Smith SM, Jenkinson M, Johansen-Berg H, Rueckert D, Nichols TE, Mackay CE, Watkins KE, Ciccarelli O, Cader MZ, Matthews PM, Behrens TE. Tract-based spatial statistics: voxelwise analysis of multi-subject diffusion data. *Neuroimage*. 2006; 31:1487–1505. [PubMed: 16624579]
56. Lie C-H, Specht K, Marshall JC, Fink GR. Using fMRI to decompose the neural processes underlying the Wisconsin Card Sorting Test. *NeuroImage*. 2006; 30:1038–1049. [PubMed: 16414280]
57. Moll J, de Oliveira-Souza R, Moll FT, Bramati IE, Andreiuolo PA. The cerebral correlates of set-shifting: an fMRI study of the trail making test. *Arquivos de neuro-psiquiatria*. 2002; 60:900–905. [PubMed: 12563376]
58. Oishi K, Zilles K, Amunts K, Faria A, Jiang H, Li X, Akhter K, Hua K, Woods R, Toga AW, Pike GB, Rosa-Neto P, Evans A, Zhang J, Huang H, Miller MI, van Zijl PC, Mazziotta J, Mori S. Human brain white matter atlas: identification and assignment of common anatomical structures in superficial white matter. *Neuroimage*. 2008; 43:447–457. [PubMed: 18692144]

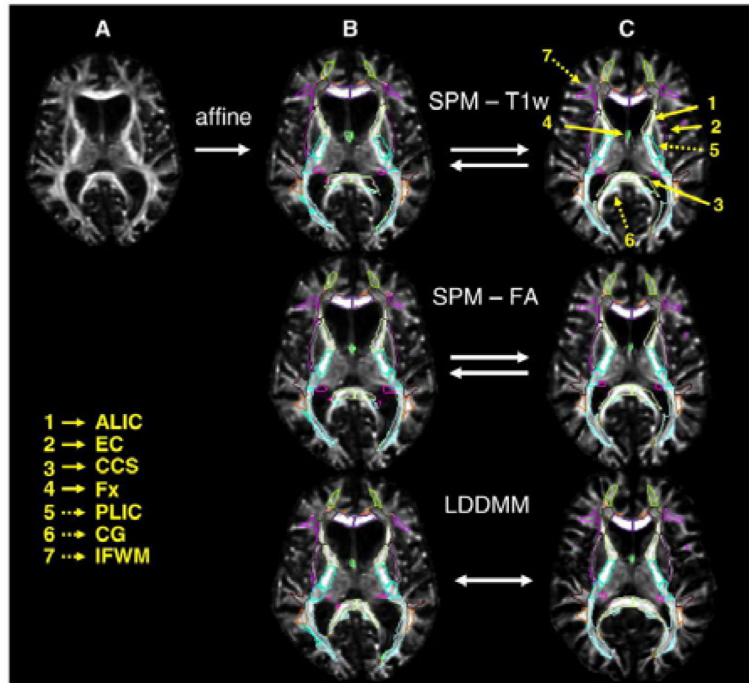


**Figure 1.**  
Image transformation and normalization to atlas using LDDMM

**Table 1**Baseline demographic and executive functioning characteristics by diagnostic group<sup>1</sup>

	NC n=25	MCI (SD) n=22	AD (SD) n=19	F	P
Age, Mean (SD)	74.3 (7.1)	75.3 (5.4)	75.1 (6.6)	0.15	0.864
Female, n (%)	14 (56%)	7 (31.82%)	4 (21.05%)		0.051
Education	16.2 (2.6)	16.0 (3.0)	15 (3.8)	0.15	0.864
CDR	0.02 (0.1)	0.47 (0.1)	1.1 (0.4)	106.3	<0.001
CDR Sum of Boxes	0.02 (0.1)	1.32 (0.81)	6.2 (2.5)	107.2	<0.001
MMSE	28.8 (1.2)	26.6 (2.1)	22.0 (3.3)	49.4	<0.001
TMT A	35.5 (13.9)	42.1 (13.8)	77.8 (39.2)	18.46	<0.001
TMT B	83.6 (34.9)	122 (71.0)	247.7 (87.3)	35.45	<0.001
Letter Fluency "F"	16.3 (4.0)	12.8 (4.5)	8.4 (4.6)	17.64	<0.001
Letter Fluency "A"	13.8 (4.1)	10.7 (4.5)	8.1 (4.9)	9.1	<0.001
Letter Fluency "S"	16.6 (4.3)	13.9 (5.9)	9.6 (6.1)	8.95	<0.001
Category Fluency Animals	20.2 (3.7)	17.2 (5.8)	10.6 (5.6)	19.8	<0.001
Category Fluency Vegetables	14.48 (3.6)	12.0 (4.4)	7.5 (3.4)	18.3	<0.001

<sup>1</sup> CDR=Clinical Dementia Rating; MMSE=Mini-mental State Examination; TMT=Trails Making Test

Table 2

Between group differences in FA: frontal parietal, cerebellum

Region	df	F	NC mean (SE) MCI mean (SE) AD mean (SE)	P	Bonferroni-corrected two-way comparisons within each region
			0.12 (2.17e-3)		
			0.12 (1.98e-3)		
Left Gyrus Rectus	2	0.01	0.12 (2.73e-3)	0.994	
			<b>0.37 (2.23e-3)</b>		
			<b>0.37 (2.89e-3)</b>		
Left Superior Frontal Gyrus White Matter	2	6.55	<b>0.36 (3.79e-3)</b>	<b>0.003</b>	<b>0.002 (NC-AD)</b>
			<b>0.34 (2.24e-3)</b>		
			<b>0.34 (2.75e-3)</b>		
Left Medial Frontal Gyrus White Matter	2	5.69	<b>0.33 (3.49e-3)</b>	<b>0.005</b>	<b>0.016 (NC-AD), 0.010 (MCI-AD)</b>
			0.34 (2.48e-3)		
			0.34 (3.12e-3)		
Left Inferior Frontal Gyrus White Matter	2	3.51	0.33 (4.68e-3)	0.036	
			0.32 (2.18e-3)		
			0.31 (3.05e-3)		
Left Lateral Fronto-Orbital Gyrus White Matter	2	4.89	0.30 (2.97e-3)	0.010	
			0.31 (1.54e-3)		
			0.32 (1.80e-3)		
Left Middle Fronto-Orbital Gyrus White Matter	2	2.18	0.31 (2.76e-3)	0.121	
			0.12 (2.17e-3)		
			0.12 (1.98e-3)		
Left Gyrus Rectus White Matter	2	0.15	0.12 (2.74e-3)	0.865	
			0.13 (1.92e-3)		
			0.13 (1.79e-3)		
Right Gyrus Rectus	2	0.85	0.14 (2.94e-3)	0.434	
			0.36 (2.21e-3)		
Right Superior Frontal Gyrus White Matter	2	4.13	0.36 (2.75e-3)	0.021	



Region	df	F	NC mean (SE) MCI mean (SE) AD mean (SE)	P	Bonferroni-corrected two-way comparisons within each region
			0.37 (2.21e-3)		
			<b>0.34 (1.88e-3)</b>		
			<b>0.33 (2.34e-3)</b>		
Right Middle Frontal Gyrus White Matter	2	8.78	<b>0.32 (3.37e-3)</b>	<0.001	<0.001 (NC-AD)
			<b>0.35 (2.07e-3)</b>		
			<b>0.34 (3.58e-3)</b>		
Right Inferior Frontal Gyrus White Matter	2	8.27	<b>0.33 (3.78e-3)</b>	0.001	<0.001 (NC-AD)
			0.31 (2.17e-3)		
			0.30 (2.32e-3)		
Right Lateral Fronto-Orbital gyrus White Matter	2	2.67	0.30 (2.75e-3)	0.077	
			0.30 (1.42e-3)		
			0.30 (1.71e-3)		
Right Middle Fronto-Orbital Gyrus White Matter	2	0.22	0.30 (2.38e-3)	0.803	
			0.31 (1.85e-3)		
			0.31 (2.25e-3)		
Right Gyrus Rectus White Matter	2	1.90	0.30 (3.24e-3)	0.158	
			<b>0.37 (3.65e-3)</b>		
			<b>0.37 (3.39e-3)</b>		
Left Superior Parietal Gyrus White Matter	2	7.28	<b>0.35 (4.24e-3)</b>	0.001	0.002 (NC-AD), 0.014 (AD-MCI)
			<b>0.35 (2.84e-3)</b>		
			<b>0.34 (3.78e-3)</b>		
Left Angular Gyrus White Matter	2	6.00	<b>0.33 (4.46e-3)</b>	0.004	0.003 (NC-AD)
			0.32 (2.55e-3)		
			0.32 (2.92e-3)		
Left Pre-cuneus White Matter	2	2.45	0.31 (2.80e-3)	0.094	
			0.32 (1.96e-3)		
			0.32 (1.87e-3)		
Left Supramarginal Gyrus White Matter	2	4.04	0.31 (2.76e-3)	0.022	

Region	df	F	NC mean (SE) MCI mean (SE) AD mean (SE)	P	Bonferroni-corrected two-way comparisons within each region
Right Superior Parietal Gyrus White Matter	2	6.75	<u>0.36 (4.42e-3)</u> <u>0.37 (4.34e-3)</u> <u>0.38 (3.02e-3)</u>	<b>0.002</b>	<b>0.002 (NC-AD)</b>
Right Angular Gyrus White Matter	2	4.66	<u>0.35 (2.74e-3)</u> <u>0.34 (3.32e-3)</u> <u>0.33 (3.34e-3)</u>	0.013	
Right Pre-cuneus White Matter	2	3.04	<u>0.32 (2.51e-3)</u> <u>0.32 (2.59e-3)</u> <u>0.31 (2.44e-3)</u>	0.055	
Right Supramarginal Gyrus White Matter	2	0.24	<u>0.33 (2.01e-3)</u> <u>0.34 (2.91e-3)</u> <u>0.33 (3.89e-3)</u>	0.788	
Left Cingulate Gyrus White Matter	2	2.76	<u>0.33 (1.75e-3)</u> <u>0.33 (2.02e-3)</u> <u>0.33 (1.76e-3)</u>	0.071	
Right Cingulate Gyrus White Matter	2	0.76	<u>0.33 (1.76e-3)</u> <u>0.33 (2.02e-3)</u> <u>0.33 (2.25e-3)</u>	0.473	
Left Cerebellum	2	0.16	<u>0.15 (2.16e-3)</u> <u>0.15 (2.71e-3)</u> <u>0.15 (2.16e-3)</u>	0.852	
Right Cerebellum	2	0.12	<u>0.16 (2.43e-3)</u> <u>0.15 (2.49e-3)</u> <u>0.15 (4.41e-3)</u>	0.883	
Left Pons	2	0.45	<u>0.28 (4.56e-3)</u> <u>0.29 (6.07e-3)</u> <u>0.28 (5.28e-3)</u>	0.640	
Right Pons	2	0.97	<u>0.35 (4.88e-3)</u>	0.385	

Region	NC mean (SE)	MCI mean (SE)	AD mean (SE)	df	F	P	Bonferroni-corrected two-way comparisons within each region
	0.35 (5.15e-3)						
	0.35 (05.71e-3)						

Table 3

Between group differences in MD: Frontal, Parietal, Cerebellum

Region	df	F	NC mean (SE) MCI mean (SE) AD mean (SE)	P	Bonferroni-corrected two-way comparisons within each region
			<b>1.18e-3 (6.21e-6)</b>		
			<b>1.17e-3 (8.48e-6)</b>		
Left Superior Frontal Gyrus	2	5.91	<b>1.21e-3 (8.73e-6)</b>	<b>0.005</b>	<b>0.025 (NC-AD), 0.006 (MCI-AD)</b>
			<b>1.18e-3 (7.67e-6)</b>		
			<b>1.18e-3 (11.0e-6)</b>		
Left Middle Frontal Gyrus	2	7	<b>1.22e-3 (11.0e-6)</b>	<b>0.002</b>	<b>0.004 (NC-AD), 0.005 (MCI-AD)</b>
			<b>1.09e-3 (7.25e-6)</b>		
			<b>1.10e-3 (9.11e-6)</b>		
Left Inferior Frontal Gyrus	2	6.41	<b>1.13e-3 (9.34e-6)</b>	<b>0.003</b>	<b>0.003 (NC-AD), 0.023 (MCI-AD)</b>
			0.82e-3 (7.47e-6)		
			0.82e-3 (6.78e-6)		
Left Superior Frontal Gyrus White Matter	2	4.09	0.85e-3 (12.2e-6)	0.021	
			0.82e-3 (7.4e-6)		
			0.81e-3 (7.83e-6)		
Left Middle Frontal Gyrus White Matter	2	4.80	0.85e-3 (11.3e-6)	0.011	
			0.82e-3 (7.65e-6)		
			0.83e-3 (9.79e-6)		
Left Inferior Frontal Gyrus White Matter	2	3.89	0.862e-3 (12.5e-6)	0.025	
			1.11e-3 (8.97e-6)		
			1.13e-3 (13.5e-6)		
Left Lateral Fronto-Orbital Gyrus	2	3.01	1.16e-3 (16.0e-6)	0.056	
			<b>1.09e-3 (10.8e-6)</b>		
			<b>1.12e-3 (13.9e-6)</b>		
Left Middle Fronto-Orbital Gyrus	2	5.48	<b>1.15e-3 (17.9e-6)</b>	<b>0.006</b>	<b>0.005 (NC-AD)</b>
Left Lateral Fronto-Orbital Gyrus White Matter	2	2.67	0.86e-3 (8.57e-6)	0.077	

Region	df	F	NC mean (SE) MCI mean (SE) AD mean (SE)	P	Bonferroni-corrected two-way comparisons within each region
			0.87e-3 (12.7e-6) 0.89e-3 (13.5e-6)		
			0.88e-3 (9.47e-6) 0.89e-3 (12.3e-6)		
Left Middle Fronto-Orbital Gyrus White Matter	2	2.68	0.92e-3 (17.6e-6)	0.076	
			<b>1.12e-3 (11.5e-6)</b> <b>1.12e-3 (12.9e-6)</b>		
Left Gyrus Rectus	2	5.50	<b>1.18e-3 (17.0e-6)</b>	<b>0.006</b>	<b>0.008 (NC-AD), 0.030 (MCI-AD)</b>
			0.87e-3 (7.63e-6) 0.87e-3 (12.4e-6)		
Left Gyrus Rectus White Matter	2	2.61	0.90e-3 (14.4e-6)	0.081	
			1.17e-3 (6.64e-6) 1.16e-3 (8.72e-6)		
Right Superior Frontal Gyrus	2	4.42	1.20e-3 (12.4e-6)	0.016	
			<b>1.15e-3 (8.57e-6)</b> <b>1.15e-3 (10.2e-6)</b>		
Right Middle Frontal Gyrus	2	5.55	<b>1.20e-3 (13.5e-6)</b>	<b>0.006</b>	<b>0.014 (NC-AD), 0.014 (MCI-AD)</b>
			1.08e-3 (9.33e-6) 1.08e-3 (8.22e-6)		
Right Inferior Frontal Gyrus	2	4.62	1.12e-3 (12.9e-6)	0.013	
			1.17e-3 (6.64e-6) 1.16e-3 (8.72e-6)		
Right Superior Frontal Gyrus White Matter	2	3.34	1.20e-3 (12.4e-6)	0.042	
			1.15e-3 (8.57e-6) 1.15e-3 (10.2e-6)		
Right Middle Frontal Gyrus White Matter	2	4.00	1.19e-3 (13.5e-6)	0.023	
			1.08e-3 (9.33e-6) 1.08e-3 (8.22e-6)		
Right Inferior Frontal Gyrus White Matter	2	3.65	1.08e-3 (8.22e-6)	0.032	

Region	df	F	NC mean (SE) MCI mean (SE) AD mean (SE)	P	Bonferroni-corrected two-way comparisons within each region
			1.12e-3 (12.9e-6)		
			1.11e-3 (9.82e-6)		
			1.11e-3 (11.1e-6)		
Right Lateral Fronto-Orbital Gyrus	2	4.35	1.16e-3 (19.1e-6)	0.017	
			1.07e-3 (11.0e-6)		
			1.09e-3 (12.6e-6)		
Right Middle Fronto-Orbital Gyrus	2	4.05	1.14e-3 (25.0e-6)	0.022	
			0.87e-3 (21.8e-6)		
			0.84e-3 (7.87e-6)		
Right Lateral Fronto-Orbital Gyrus White Matter	2	1.13	0.84e-3 (9.72e-6)	0.329	
			0.87e-3 (10.3e-6)		
			0.87e-3 (12.1e-6)		
Right Middle Fronto-Orbital Gyrus White Matter	2	0.63	0.89e-3 (21.2e-6)	0.534	
			1.10e-3 (10.4e-6)		
			1.11e-3 (11.9e-6)		
Right Gyrus Rectus	2	8.35	1.17e-3 (17.6e-6)	<0.001	0.010 (NC-AD), 0.007 (MCI-AD)
			0.86e-3 (7.98e-6)		
			0.86e-3 (9.97e-6)		
Right Gyrus Rectus White Matter	2	6.10	0.92e-3 (21.9e-6)	0.0034	0.007 (NC-AD), 0.012 (MCI-AD)
			1.13e-3 (8.51e-6)		
			1.12e-3 (11.7e-6)		
Left Superior Parietal Gyrus	2	1.25	1.15e-3 (12.9e-6)	0.293	
			0.82e-3 (11.4e-6)		
			0.80e-3 (6.70e-6)		
Left Superior Parietal Gyrus White Matter	2	2.76	0.83e-3 (14.6e-6)	0.071	
			1.21e-3 (14.1e-6)		
			1.20e-3 (18.4e-6)		
Left Pre-cuneus	2	1.10	1.23e-3 (18.0e-6)	0.338	



Region	df	F	NC mean (SE) MCI mean (SE) AD mean (SE)	P	Bonferroni-corrected two-way comparisons within each region
Left Pre-cuneus White Matter	2	3.28	0.82e-3 (13.1e-6)	0.044	
			0.81e-3 (9.73e-6)		
			0.86e-3 (18.3e-6)		
Left Supramarginal Gyrus	2	3.71	1.16e-3 (11.5e-6)	0.030	
			1.15e-3 (12.0e-6)		
			1.20e-3 (13.5e-6)		
Left Supramarginal Gyrus White Matter	2	4.37	0.82e-3 (8.27e-6)	0.017	
			0.81e-3 (7.08e-6)		
			0.85e-3 (12.7e-6)		
Left Angular Gyrus	2	1.93	1.14e-3 (11.5e-6)	0.153	
			1.15e-3 (13.4e-6)		
			1.18e-3 (15.5e-6)		
Left Angular Gyrus White Matter	2	2.70	0.81e-3 (10.5e-6)	0.075	
			0.80e-3 (9.07e-6)		
			0.84e-3 (17.7e-6)		
Right Superior Parietal Gyrus	2	1.15	1.14e-3 (7.71e-6)	0.322	
			1.13e-3 (9.13e-6)		
			1.15e-3 (9.83e-6)		
Right Superior Parietal Gyrus White Matter	2	2.23	0.82e-3 (14.1e-6)	0.116	
			0.79e-3 (7.36e-6)		
			0.80e-3 (9.97e-6)		
Right Pre-cuneus	2	1.83	1.26e-3 (11.8e-6)	0.169	
			1.25e-3 (16.2e-6)		
			1.28e-3 (11.9e-6)		
Right Pre-cuneus White Matter	2	1.82	0.81e-3 (17.1e-6)	0.170	
			0.79e-3 (11.7e-6)		
			0.83e-3 (15.2e-6)		
Right Supramarginal Gyrus	2	2.44	0.81e-3 (7.48e-6)	0.095	

Region	df	F	NC mean (SE) MCI mean (SE) AD mean (SE)	P	Bonferroni-corrected two-way comparisons within each region
			0.80e-3 (5.91e-6) 0.83e-3 (1.7e-6)		
			1.13e-3 (10.8e-6) 1.14e-3 (10.3e-6)		
Right Supramarginal Gyrus White Matter	2	3.05	1.16e-3 (11.2e-6)	0.055	
			<b>1.14e-3 (13.8e-6)</b> <b>1.13e-3 (11.5e-6)</b>		
Right Angular Gyrus	2	5.91	<b>1.20e-3 (15.7e-6)</b>	<b>0.004</b>	<b>0.017 (NC-AD), 0.007 (MCI-AD)</b>
			0.79e-3 (8.72e-6) 0.78e-3 (8.34e-6)		
Right Angular Gyrus White Matter	2	2.67	0.81e-3 (14.7e-6)	0.077	
			<b>1.15e-3 (10.2e-6)</b> <b>1.14e-3 (13.3e-6)</b>		
Left Cingulate Gyrus	2	6.82	<b>1.19e-3 (12.7e-6)</b>	<b>0.002</b>	<b>0.004 (NC-AD), 0.009 (MCI-AD)</b>
			<b>0.85e-3 (9.11e-6)</b> <b>0.86e-3 (10.3e-6)</b>		
Left Cingulate Gyrus white Matter	2	9.26	<b>0.92e-3 (13.8e-6)</b>	<b>&lt;0.001</b>	<b>0.000 (NC-AD), 0.003 (MCI-AD)</b>
			1.21e-3 (10.3e-6) 1.21e-3 (12.6e-6)		
Right Cingulate Gyrus	2	4.81	1.26e-3 (14.4e-6)	0.011	
			<b>0.90e-3 (9.73e-6)</b> <b>0.90e-3 (11.8e-6)</b>		
Right Cingulate Gyrus White Matter	2	6.80	<b>0.95e-3 (17.4e-6)</b>	<b>0.002</b>	<b>0.009 (NC-AD), 0.004 (MCI-AD)</b>
			1.05e-3 (9.89e-6) 1.04e-3 (9.86e-6)		
Left Cerebellum	2	2.02	1.07e-3 (9.25e-6)	0.141	
			1.04e-3 (10.1e-6) 1.03e-3 (11.1e-6)		
Right Cerebellum	2	0.51	1.03e-3 (11.1e-6)	0.604	

Region	df	F	NC mean (SE) MCI mean (SE) AD mean (SE)	P	Bonferroni-corrected two-way comparisons within each region
			1.05e-3 (9.34e-6)		
			0.91e-3 (8.17e-6)		
			0.92e-3 (11.8e-6)		
Left Pons	2	0.52	0.92e-3 (13.4e-6)	0.597	
			0.96e-3 (7.74e-6)		
			0.97e-3 (13.6e-6)		
Right Pons.	2	0.81	0.98e-3 (12.6e-6)	0.451	

Table 4

Within group linear regression: FA

Region <sup>2</sup>	L_SFWM	L_MFWM	R_MFWM	R_IFWM	L_SPWM	L_AWM	R_SPWM	R_AWM	R_PONS	L_PONS
<b>b</b>	43.49	37.14	46.46	39.36	21.98	19.24	38.23	8.24	-0.52	1.80
<b>Eta<sup>2</sup></b>	0.26	0.14	0.25	0.24	0.10	0.07	0.21	0.01	<0.01	<0.01
<b>SE</b>	19.02	23.97	20.96	18.11	18.10	17.82	18.97	26.54	14.51	13.20
<b>95% CI</b>	2.94, 84.03	-13.96, 88.24	1.79, 91.12	0.77, 77.95	-16.60, 60.55	-18.74, 57.22	-2.21, 78.67	-48.34, 64.82	-31.44, 30.41	-26.34, 29.94
<b>P</b>	<b>0.037</b>	0.142	<b>0.043</b>	<b>0.046</b>	0.243	0.297	0.062	0.761	0.972	0.894
<b>b</b>	33.04	38.97	31.90	25.82	11.90	28.70	3.80	20.91	9.50	14.17
<b>Eta<sup>2</sup></b>	0.30	0.35	0.18	0.30	0.05	0.39	0.01	0.17	0.11	0.17
<b>SE</b>	11.90	12.50	16.12	9.38	11.87	8.42	9.86	11.06	6.45	7.32
<b>95% CI</b>	8.03, 58.04	12.71, 65.22	-1.97, 65.77	6.10, 45.53	-13.04, 36.84	11.01, 46.39	-16.90, 24.50	-2.33, 44.15	-4.06, 23.07	-1.20, 29.55
<b>P</b>	<b>0.012</b>	<b>0.006</b>	0.063	<b>0.013</b>	0.329	<b>0.003</b>	0.704	0.075	0.158	0.069
<b>b</b>	0.28	11.14	8.99	14.22	4.02	-1.94	1.84	4.57	1.60	0.56
<b>Eta<sup>2</sup></b>	<0.01	0.07	0.03	0.09	0.02	<0.01	<0.01	0.02	0.01	<0.01
<b>SE</b>	9.57	8.97	11.01	9.65	5.54	7.22	6.78	7.48	4.55	4.19
<b>95% CI</b>	-19.62, 20.20	-7.52, 29.81	-13.90, 31.89	-5.84, 34.28	-7.50, 15.55	-16.96, 13.07	-12.26, 15.95	-10.98, 20.13	-3.97, 3.45	-8.16, 9.28
<b>P</b>	0.976	0.228	0.423	0.155	0.476	0.790	0.788	0.547	0.728	0.896

<sup>2</sup> L\_SFWM= Left Superior Frontal Gyrus White Matter; L\_MFWM= Left Medial Frontal Gyrus White Matter; L\_LFWM= Left Lateral Frontal Gyrus White Matter; R\_MFWM= Right Middle Frontal Gyrus White Matter; R\_IFWM= Right Inferior Frontal Gyrus White Matter; L\_SPWM=Left Superior Parietal Gyrus White Matter; L\_AWM= Left Angular Gyrus White Matter; R\_SPWM= Right Superior Parietal Gyrus White Matter; R\_AWM= Right Angular Gyrus White Matter; L\_PONS= Left Pons; R\_PONS= Right Pons. Models adjusted for age and education.